

Development of Soil Temperature Profile and Tipping Bucket with Datalogger

¹Alamuoye H.I. ²Ewetumo T. ³Okunlola B. A. ⁴Bello R O. and ⁵Joseph-Ojo C. A.

^{1,2,4,5} Department of Physics (Electronics and Energy), FUT, Akure

³Department of Department of Meteorology and Climate Science, FUT, Akure

DOI: <https://doi.org/10.56293/IJASR.2022.5518>

IJASR 2023

VOLUME 6

ISSUE 3 MAY – JUNE

ISSN: 2581-7876

Abstract: In a savanna climate, the soil surface is tilled solely to reduce evaporation during the dry summer period. Where models exist for predicting water and heat movement through soils, soil conductivity, thermal diffusivity, and soil bulk density are required. To overcome difficult physical properties of soil, the soil temperature measurement was designed and built directly and accurately with locally sourced materials. Six semiconductor temperature (DS18B20) sensors, a tipping bucket, a graphic display, a real-time clock, a microSD card shield, and a microcontroller comprise the device (arduino mega 2560). The temperature sensor has a resolution of 0.0625 °C and a maximum temperature of 120 °C, making it suitable for measuring soil temperature. The tipping bucket has 0.2794 mm per tipping and a real switch time of 1 ms. The log of the datalogger.

Keywords: Soil, Temperature profile, tipping bucket,

1. Introduction

The soil surface is sometimes tilled in Savanna climates to reduce evaporation during the dry summer period. While there are models that predict how water and heat move through soils, they typically require knowledge of unsaturated hydraulic conductivity, thermal diffusivity, and soil bulk density. Tillage alters soil porosity, average void size, surface roughness, and other conditions that influence heat and water movement. Under these conditions, soil temperature can be measured directly and accurately. Currently, efforts are being made to estimate the more difficult-to-measure hydraulic properties based on the spatial distribution of temperature waves produced by the sun on a daily basis [1, 2, 3, 4]. The ease with which high resolution temperature profiles can be produced in the field will, to a large extent, determine how quickly these efforts are developed and implemented.

Because they are reliable, stable, and can be recorded with automated equipment, thermocouples or thermistors are commonly used as temperature sensors. Thermocouple has temperature drift and a complex circuit for accurate reading, while thermistor is nonlinear and requires careful experimentation to generate a linearization equation. If the reference voltage varies, the output voltage representation will deviate from calibration. An individual thermocouple or thermistor installed at the end of a cable is the most common configuration. These can be inserted at any desired depth, but unless the connecting cables are extremely thin, they should be run horizontally for several centimeters at the same depth to ensure heat from other depths is not conducted through the wire, especially at installations near the surface. To accomplish this, sensors are frequently installed by digging a trench and inserting the sensors into the trench's side.

It is difficult to ensure that the vertical spacing remains precise and constant throughout the experiment when installing individual sensors. It is also difficult to install sensors at close intervals without disturbing the soil within the measurement zone. Sensors can be placed farther apart horizontally to allow for smaller vertical spacing, but temperature profiles at different locations may differ due to spatial differences in the soil surface.

We developed a method for building solid arrays of semiconductor temperature sensors to make it feasible to produce numerous detailed temperature profiles under both tilled and untilled surface conditions. The goal was to be able to drive the array into the soil with a mallet and then record temperatures at 1-cm intervals down to a depth of 20 cm or less, and 5-cm intervals down to a depth of 45 cm [5, 6, 7].

The basic electronic design of such an array has previously been described [8]. The temperature sensor is made up of thermistors, and a datalogger is used to measure the voltage drop and current across each thermistor, from which the resistance is calculated. A thermistor's resistance is directly and predictably related to its temperature. What has not previously been described is a practical method for constructing an array of temperature sensors spaced at regular intervals that is strong enough to withstand being driven into the soil with a mallet. We are also unaware of any tests that have been conducted to determine how accurately such a device estimates surface and near-surface temperatures, despite the fact that the device may transmit heat more readily than soil.

On this researcher's semiconductor temperature sensor, temperature of the soil was measured directly with border measuring current and voltage before conversion. A datalogger was built to record temperature in real time while measuring the amount of water from the rain or sprinkler

2. Materials and Method

Figure 1 shows a block diagram of the soil temperature profile and tipping bucket for measuring rain volume or water sprinkler volume. The semiconductor temperature used in this study is DS18B20, and the tipping bucket is from Sparkfun.

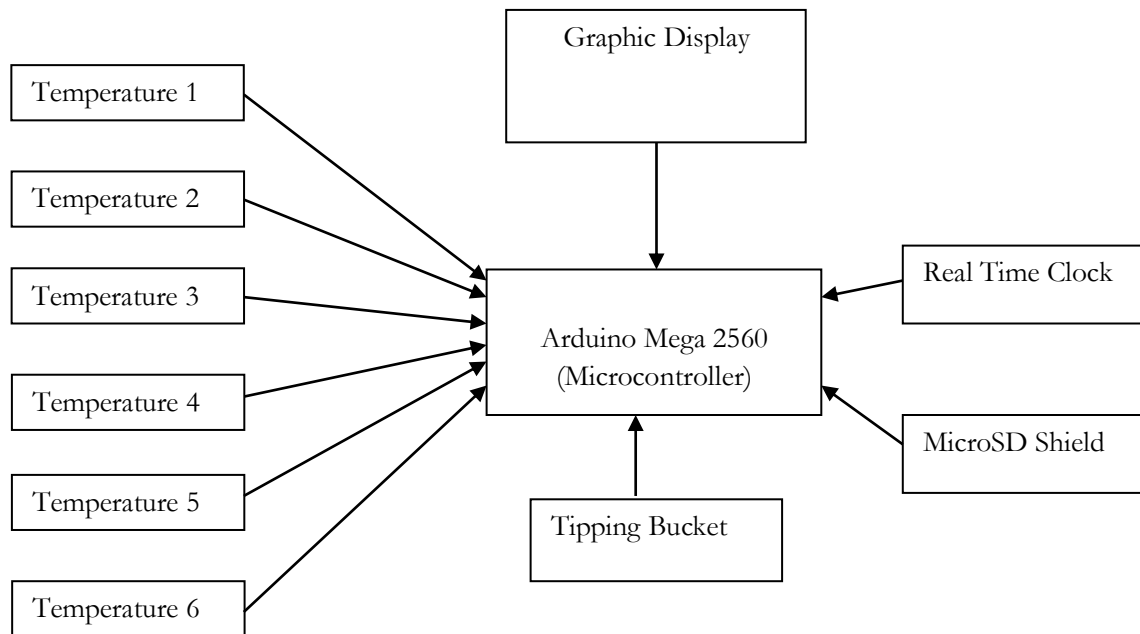


Figure 1. Block Diagram of Soil Profile Measurement

3. Semiconductor Temperature Sensor (DS18B20)

The DS18B20 is a direct-to-digital temperature sensor. The resolution of the temperature sensor is user-configurable to 9, 10, 11, or 12 bits, corresponding to increments of 0.5°C, 0.25°C, 0.125°C, and 0.0625°C, respectively. The default resolution at power-up is 12-bit. The DS18B20 powers up in a low-power idle state. To initiate a temperature measurement and A-to-D conversion, the master must issue a Convert T [44h] command. Following the conversion, the resulting thermal data is stored in the 2-byte temperature register in the scratchpad memory and the DS18B20 returns to its idle state. If the DS18B20 is powered by an external supply, the master can issue “read time slots” after the Convert T command and the DS18B20 will respond by transmitting 0 while the temperature conversion is in progress and 1 when the conversion is done. If the DS18B20 is powered with parasite power, this notification technique cannot be used since the bus must be pulled high by a strong pull-up during the entire temperature conversion. Figure 2 shows the internal block diagram of DS18B20

The wire of DS18B20 was inserted into a copper pipe of 4 mm welded and then sealed at one end using gas welding with brass soldering material at the other end after inserted the temperature a silicon gum is used to seal it to prevent water from entering into the DS18B20 temperature sensor.

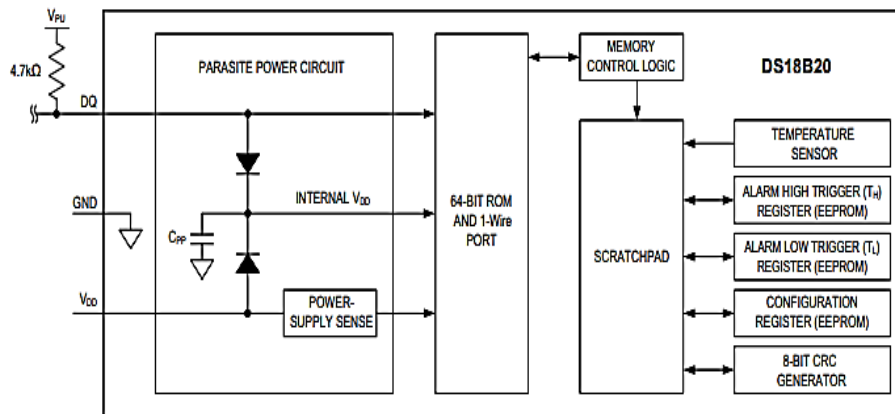


Figure 2: Block diagram of DS1820B Temperature Sensor

4. MicroSD Card Shield

SD card reader module is interfaced with the microcontroller with SPI (Serial Peripheral interface) standard. The module is designed for dual voltage power supply. The interface module can be used with two logic level either CMOS 3.3V or TTL 5V, as shown on Figure 3 of the schematic diagram of MicroSD card. [9]

5. Real Time Clock

The DS3232 is a low-cost temperature-compensated crystal oscillator (TCXO) with a very accurate, temperature-compensated, integrated real-time clock (RTC) and 236 bytes of battery-backed SRAM. Additionally, the DS3232 incorporates a battery input and maintains accurate timekeeping when main power to the device is interrupted. The integration of the crystal resonator enhances the long-term accuracy of the device as well as reduces the piece-part count in a manufacturing line.

6. The RTC maintains seconds, minutes, hours, day, date, month, and year information.

The date at the end of the month is automatically adjusted for months with fewer than 31 days, including corrections for leap year. The clock operates in either the 24-hour or 12-hour format with an AM/PM indicator. Two programmable time-of day alarms and a programmable square-wave output are provided. Address and data are transferred serially through an I2C bidirectional bus. The schematic diagram of RTC is shown in Figure 4.

7. Range Gauge (Tipping Bucket)

The rain gauge tipping bucket in Figure 5 consists of a funnel, tipping lever, volume adjuster, rain water outlet, enclosure tube and base. The volume adjustable stopper was incorporated on either side of the lever. This allows to adjust the resolution of tipping bucket could be varied from 10 ml to 50 ml. When a magnet pass over the reel switch could count tips of the lever in both directions.

The rain gauge used was made of plastic and measured 14.8cm x 6cm x 8.1cm (Figure 6). When a magnet passes over it, it activates a microcontroller via a reel switch. The trigger will count the number of tipping lever tips and convert them to the equivalent volume of liquid when the lever is adjusted for a tip. The tipping bucket is permanently attached to the adjuster. The rain gauge bucket has a 0.011" (0.2794 mm) rain capacity holding recordable by microcontroller interrupting input before tipping. The switch on the gauge is linked to the resistor capacitor network (Figure 7).

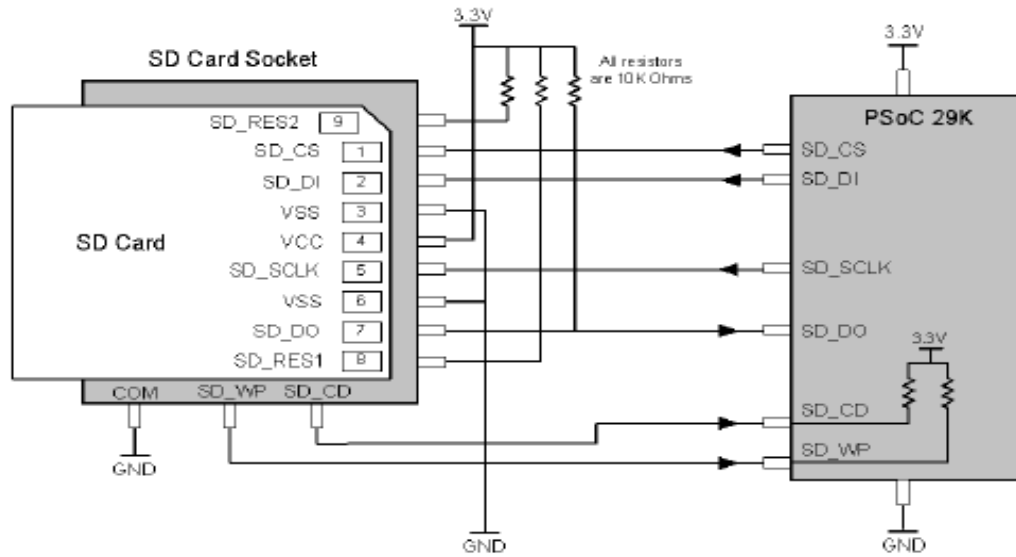


Figure 3. Schematic Diagram of MicroSD Card Module

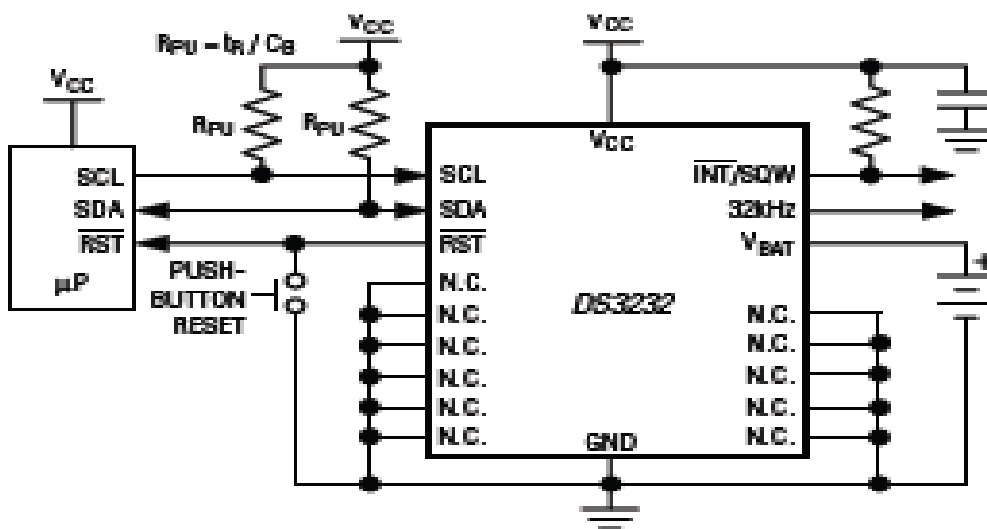


Figure 4. Schematic Diagram of RTC

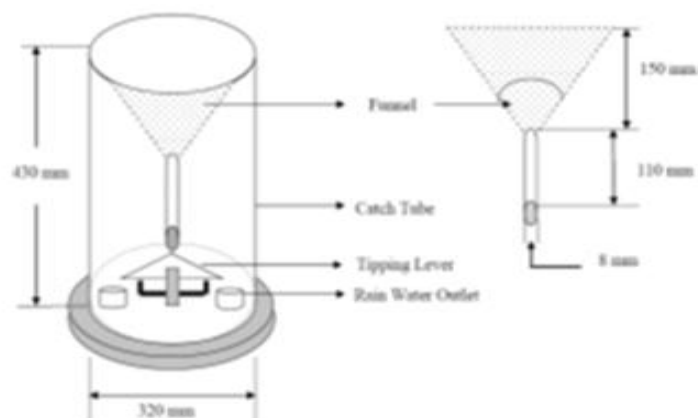


Figure 5. Schematic Diagram of Tipping Bucket



Figure 6: Tipping Bucket (Rain Gauge Bucket)

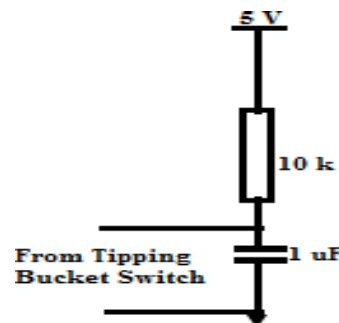


Figure 7. Circuit of Connection

8. Microcontroller Unit with Logging and Display Unit

Microcontroller is small size computer on a single IC containing processor core, memory and programmable input-output peripheral. Microcontrollers are designed for the use of embedded applications, in contrast with microprocessor which are used for personal computers and other general purpose applications. Atmega2560 is a low power, high performance; CMOS 8-bit microcontroller based on the AVR enhanced RISC architecture. Atmega2560 provides 256 Kbytes with 8 Kbyte RAM of in-system self-programmable memory with read while write capability and 2 Kbyte EPROM. The microcontroller coordinates all the activities of the instrument from accepting data from load cell amplifier to the processing of data to the storing and displaying information.

MicroSD card shield module was interfaced with microcontroller using Serial Peripheral interface (SPI) protocol standard. The module is designed for dual voltage power supply. The interface module can be used with two logic level i.e. CMOS 3.3V or TTL 5V.

The Liquid Crystal Display (LCD) is used to display the draught force during tillage operation for visual information. A Dig chip make 20 character × 4 lines JHD162A liquid crystal display was used in the instrument developed. The display is a 16 pin which works with maximum power supply of 5.0 V and the data can be sent in either 4 bit, 2 operations or 8-bit, 1 operation so that it can be interfaced to 8-bit Microcontroller. Here we used 4 bits, 2 operation system.

10. Result and Conclusion

The device was tested in a laboratory setting, and the sensors attached performed admirably. Table 1 shows a sample of data logged by a device datalogger. If a device is deployed in the field, it can help hydrologists model soil temperature more accurately than manually collected data, which is prone to human error and error when reading a soil thermometer incorrectly.

Table1. Sample of Logging Data obtained fro Device in Laboratory

| Device for Hydrology Measurement | | | | | | | | | | |
|----------------------------------|------------|----------|-----------------------|-----------------------|-----------------------|-----------------------|-----------------------|-----------------------|------------------|--------------------|
| id | Date | Time | Temp. Level1 (deg.C) | Temp. Level2 (deg.C) | Temp. Level3 (deg.C) | Temp. Level4 (deg.C) | Temp. Level5 (deg.C) | Temp. Level6 (deg.C) | Rain Volume(mm) | Rain Rate (mm/hr) |
| 1 | 11/11/2022 | 10:48:41 | 27.19 | 27.4 | 27.25 | 27.25 | 27.19 | 27.2 | 0 | 0 |
| 2 | 11/11/2022 | 10:48:55 | 27.19 | 27.4 | 27.25 | 27.25 | 27.19 | 27.2 | 0 | 0 |
| 3 | 11/11/2022 | 10:49:09 | 27.19 | 27.4 | 27.31 | 27.25 | 27.19 | 27.2 | 0 | 0 |
| 4 | 11/11/2022 | 10:49:23 | 27.19 | 27.4 | 27.25 | 27.25 | 27.19 | 27.2 | 0 | 0 |
| 5 | 11/11/2022 | 10:49:37 | 27.19 | 27.4 | 27.25 | 27.25 | 27.19 | 27.2 | 0 | 0 |
| 6 | 11/11/2022 | 10:49:52 | 27.31 | 27.4 | 27.25 | 27.25 | 27.19 | 27.2 | 0 | 0 |
| 7 | 11/11/2022 | 10:50:06 | 27.81 | 27.4 | 27.31 | 27.31 | 27.19 | 27.2 | 0 | 0 |
| 8 | 11/11/2022 | 10:50:20 | 27.94 | 27.4 | 27.31 | 27.31 | 27.25 | 27.3 | 0 | 0 |
| 9 | 11/11/2022 | 10:50:34 | 27.94 | 27.4 | 27.31 | 27.37 | 27.25 | 27.3 | 0 | 0 |
| 10 | 11/11/2022 | 10:50:48 | 27.87 | 27.4 | 27.31 | 27.37 | 27.25 | 27.3 | 0 | 0 |
| 11 | 11/11/2022 | 10:51:03 | 27.81 | 27.4 | 27.31 | 27.37 | 27.25 | 27.3 | 0 | 0 |
| 12 | 11/11/2022 | 10:51:17 | 27.81 | 27.4 | 27.37 | 27.37 | 27.25 | 27.3 | 0 | 0 |
| 13 | 11/11/2022 | 10:51:31 | 27.75 | 27.4 | 27.37 | 27.37 | 27.25 | 27.3 | 0 | 0 |
| 14 | 11/11/2022 | 10:51:45 | 27.69 | 27.4 | 27.37 | 27.37 | 27.31 | 27.3 | 0 | 0 |
| 15 | 11/11/2022 | 10:51:59 | 27.69 | 27.5 | 27.37 | 27.37 | 27.31 | 27.3 | 0 | 0 |
| 16 | 11/11/2022 | 10:52:13 | 27.62 | 27.5 | 27.37 | 27.37 | 27.31 | 27.3 | 0 | 0 |
| 17 | 11/11/2022 | 10:52:28 | 27.62 | 27.5 | 27.37 | 27.37 | 27.31 | 27.3 | 0 | 0 |
| 18 | 11/11/2022 | 10:52:42 | 27.56 | 27.5 | 27.37 | 27.37 | 27.31 | 27.3 | 0 | 0 |
| 19 | 11/11/2022 | 10:52:56 | 27.56 | 27.5 | 27.37 | 27.37 | 27.31 | 27.3 | 0 | 0 |
| 20 | 11/11/2022 | 10:53:10 | 27.5 | 27.5 | 27.37 | 27.37 | 27.31 | 27.3 | 0 | 0 |
| 21 | 11/11/2022 | 10:53:24 | 27.5 | 27.5 | 27.37 | 27.37 | 27.31 | 27.3 | 0 | 0 |
| 22 | 11/11/2022 | 10:53:39 | 27.5 | 27.5 | 27.37 | 27.37 | 27.31 | 27.3 | 0 | 0 |

References

1. Wu, J. and Nofziger, D.L. (1999). Incorporating temperature effects on pesticide dug radiation into a management model. *J. Environ. Qual.* 28: 92-100.
2. Geiger, R., Aron, R.N. and Todhunter, P. (2003). *The climate near the ground.* Rownaan and little field publishers, Inc. Lanham, 42-50.
3. Heitman, J.L., R. Horton, T.J. Sauer, and T.M. Desutter. 2008a. Sensible heat observations reveal soil-water evaporation dynamics. *J. Hydro-meteorol.* 9:165–171. doi:10.1175/2007JHM963.1
4. Heitman, J.L., X. Xiao, R. Horton, and T.J. Sauer. 2008b. Sensible heat measurements indicating depth and magnitude of subsurface soil water evaporation. *Water Resour. Res.* 44:W00D05 10.1029/2008WR006961. doi:10.1029/2008WR006961
5. Wuest, S.B. 2010. Tillage depth and timing effects on soil water profiles in two semiarid soils. *Soil Sci. Soc. Am. J.* 74:1701–1711. doi:10.2136/sssaj2010.0046
6. Wuest S. B. (2012). An Array for Measuring Detailed Soil Temperature Profiles, *Soil Science Society of America Journal* 77:427–431 doi:10.2136/sssaj2012.0309n
<https://www.ars.usda.gov/ARUserFiles/6233/anArrayForMeasuring.pdf> (assessed on 11/17/2022, 4:13 am)
7. Ham, J.M., and R.S. Senock. 1992. On the measurement of soil surface temperature. *Soil Sci. Soc. Am. J.* 56:370–376. doi:10.2136/sssaj1992.03615995005600020006x
8. McInnes, K.J. 2002. Soil heat. In J.H. Dane and G.C. Topp, editors, *Methods of soil analysis.* Part 4. SSSA Book Ser. 5. SSSA, Madison, WI. p. 1183–1199.
9. Ewetumo, T., Egbedele I., Joseph-Ojo. I., & Fagbamiye-Akinwale, O. M.(2019): Development of Low-cost Soil Tillage Profilemeter, *Iconic Research and Engineering Journal (IRE).* India 3(2): 365- 371.